RL-TR-91-375
Final Technical Report
December 1991

DIRECT OPTICAL TO MICROWAVE CONVERSION

University of Dayton

Dr. Henry F. Taylor (Texas A&M University)

APPROVED FOR PUBLIC RELEASE; DISTRIBUTION UNLIMITED.

Rome Laboratory
Air Force Systems Command
Griffiss Air Force Base, NY 13441-5700

This report has been reviewed by the Rome Laboratory Public Affairs Office (PA) and is releasable to the National Technical Information Service (NTIS). At NTIS it will be releasable to the general public, including foreign nations.

RL-TR-91-375 has been reviewed and is approved for publication.

APPROVED: David A Garafalo

DAVID A. GARAFALO
Project Engineer

FOR THE COMMANDER: John A Graniero

JOHN A. GRANIERO
Chief Scientist
Command, Control, & Communications Directorate

If your address has changed or if you wish to be removed from the Rome Laboratory mailing list, or if the addressee is no longer employed by your organization, please notify RL(C3DB) Griffiss AFB NY 13441-5700. This will assist us in maintaining a current mailing list.

Do not return copies of this report unless contractual obligations or notices on a specific document require that it be returned.

REPORT DOCUMENTATION PAGE

Form Approved
OMB No. 0704-0188

1. AGENCY USE ONLY (Leave Blank)	2. REPORT DATE	3. REPORT TYPE AND DATES COVERED
	December 1991	Final Apr 90 - Jul 91

4. TITLE AND SUBTITLE
DIRECT OPTICAL TO MICROWAVE CONVERSION

5. FUNDING NUMBERS
C - F30602-88-D-0028,
Task C-0-2019
PE - 63726F
PR - 2853
TA - 92
WU - PN

6. AUTHOR(S)
Dr. Henry F. Taylor

7. PERFORMING ORGANIZATION NAME(S) AND ADDRESS(ES)
Texas A&M University
College Station TX 77843

8. PERFORMING ORGANIZATION REPORT NUMBER
N/A

9. SPONSORING/MONITORING AGENCY NAME(S) AND ADDRESS(ES)
Rome Laboratory (C3DB)
Griffiss AFB NY 13441-5700

10. SPONSORING/MONITORING AGENCY REPORT NUMBER
RL-TR-91-375

11. SUPPLEMENTARY NOTES
Rome Laboratory Project Engineer: David A. Garafalo/C3DB/(315) 330-4097
Prime Contractor: University of Dayton

12a. DISTRIBUTION/AVAILABILITY STATEMENT
Approved for public release; distribution unlimited.

12b. DISTRIBUTION CODE

13. ABSTRACT (Maximum 200 words)

A traveling wave (TW) photodetector with a coplanar stripline structure was designed and fabricated in semiinsulating GaAs. Ohmic Au/Ge/Ni contracts were formed by a thermal annealing process. Testing was accomplished using an optical delay line arrangement to achieve either matching or mismatching of the microwave phases of the optical inputs and the microwave output signal. For the phase-matched case, the optical inputs are coherently combined to produce the TW photodetector output. The observed average microwave output power over the frequency range 0.5-5 GHz was 11 dB greater for four identical inputs than for a single input. This compares with an ideal value of 12 dB for the power increase. For the unmatched case, the TW photodetector operates as a transversal filter, with the fundamental frequency determined by the optical/microwave time-delay mismatch. Experimentally, a fundamental frequency of 4.3 GHz was observed for two, three or four optical inputs. The expected sidelobe pattern was seen in each case.

14. SUBJECT TERMS	15. NUMBER OF PAGES
Micrwoave, optics, optoelectronics, traveling wave, photodetector	24
	16. PRICE CODE

17. SECURITY CLASSIFICATION OF REPORT	18. SECURITY CLASSIFICATION OF THIS PAGE	19. SECURITY CLASSIFICATION OF ABSTRACT	20. LIMITATION OF ABSTRACT
UNCLASSIFIED	UNCLASSIFIED	UNCLASSIFIED	UL

TABLE OF CONTENTS

INTRODUCTION

The key to many of the microwave applications of optics will be the ability to integrate photodetectors with monolithic microwave integrated circuits (MMICs). This will allow microwave signals to be coupled optically into MMICs via fiber optic lines. Such optoelectronic integrated circuits (OEICs) could have widespread application in Air Force electronic warfare and radar systems. Monolithic OEIC technology is in its infancy, and many aspects of device fabrication and application remain to be explored.

Building upon the technology base established at Texas A&M over the past several years, we have explored new possibilities for optically coupled microwave devices. In particular, a traveling wave (TW) photodetector [1] and integration of such a photodetector with other MMIC circuit elements have been investigated.

The TW photodetector is configured as a coplanar transmission line on a semiinsulating gallium arsenide substrate, as illustrated in Fig. 1. Light modulated at microwave frequencies is coupled into the stripline gap to produce electron-hole pairs. The resulting current flow in the gap produces a microwave signal on the transmission line. Phase matching of optical and microwave signals is accomplished with optical delay lines. A configuration in which the incident light is confined in two dimensions by an optical waveguide has also been explored. The TW photodetector is readily integrable with other microwave elements, such as FET amplifiers and Gunn oscillators, and its distributed nature allows higher microwave power levels to be generated than with other types of photodetector.

Results of our research on the design, fabrication, and testing of TW photodetectors are described below.

DESIGN OF TW PHOTODETECTOR

A TW photodetector with a coplanar stripline structure has been designed and fabricated. The configuration is illustrated in Fig. 2. The metallization is formed on a semi-insulating GaAs substrate which has a resistivity in the range of 10^7 Ω-cm. The electrode pattern is produced using lift-off photolithographic techniques. The metalization consists of Au-Ge/Ni layers which form the ohmic contact.

The gap between the two electrodes is the active area. The width of the gap w can be optimized by considering the focussed beam spot size. When a Gaussian optical beam is focused, the spot diameter (to e^{-2} relative power density) $2r_o$ is given by

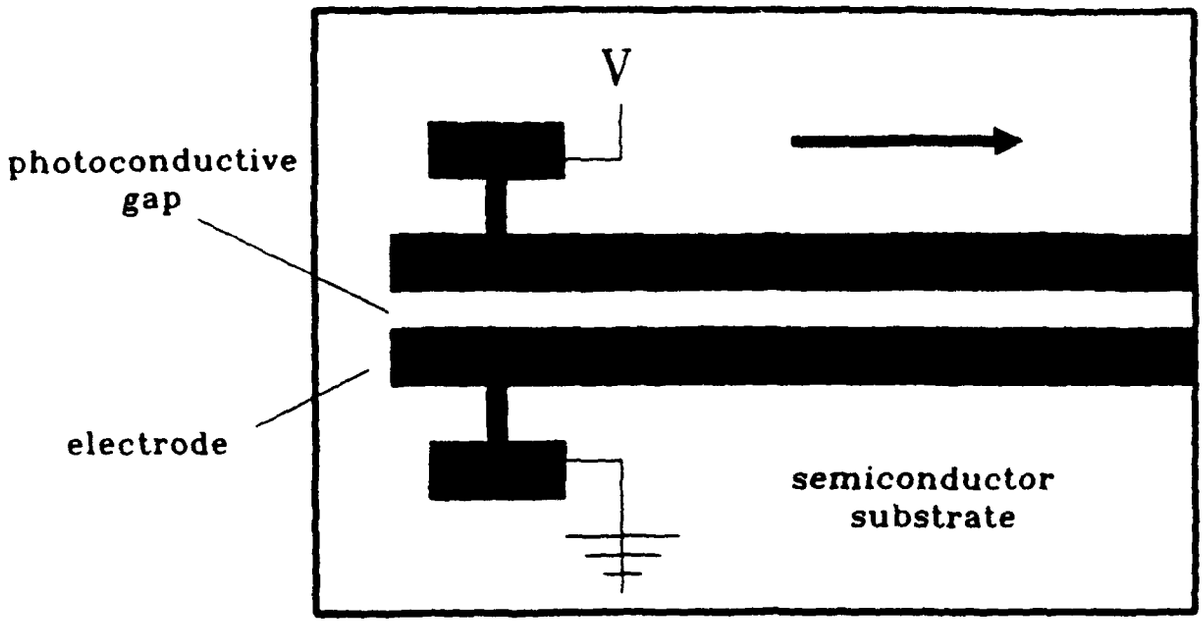

Fig. 1. Coplanar transmission line configuration for TW photodetector.

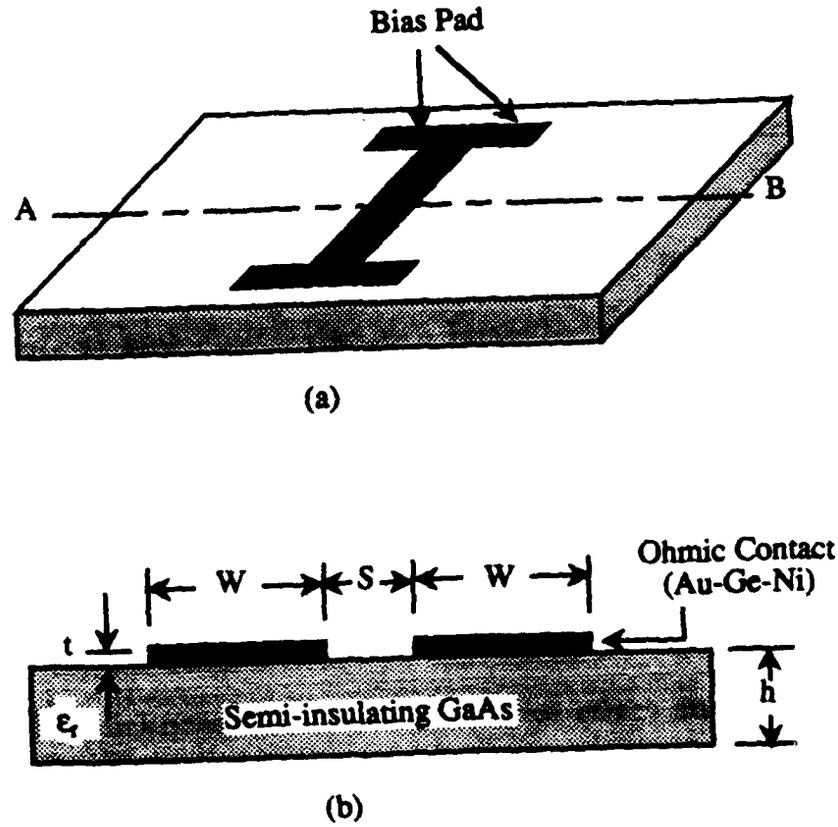

Fig. 2. TW photodetector design: (a) perspective view, (b) end view.

$$2r_o = 2.44\lambda(f/2a), \qquad (1)$$

where f is the focal length of the optical system, 2a is the diameter of the collimated optical beam, f/2a is the equivalent F-number of the optical system, and λ is the optical wavelength. The minimum spot size is thus proportional to the focal length of the lens and the wavelength of the laser source. In determining the optimum electrode gap width, it should be noted that the electrical resistance between the two striplines will be very high if the optical beam does not overlap the strip lines ($w >> 2r_0$), but optical losses will be high if most of the light falls on the electrodes ($w << 2r_0$) [2]. For Gaussian beam illumination, the optical power density distribution P(r) depends on the distance r from the center of the beam spot acording to the expression

$$P(r) = P_o \exp(-2r^2/r_o^2), \qquad (2)$$

where P_0 is the maximum power density in the center of the spot and r_0 is the radius of the focussed beam. It has been shown that the optimum gap width d_o is given by $d_o \approx 1.5r_o$ [2]. For an F-number of 2 and λ = 0.83 μm, we find from eq. (1) that r_0 = 2.0 μm. The optimum gap width is thus found to be 3.0 μm.

To interface a TW photodetector to other striplines, coaxial cable, waveguides, or MMIC components, the characteristic impedance is usually designed to be 50Ω. Analytical expressions for calculating the characteristic impedance for coplanar striplines have been reported by several authors [3]-[6]. Wen's expression [3] has a simple closed form. However, it was obtained under the assumption that the dielectric substrate is thick enough to be considered infinite, while Gupta's formula [4] only holds for moderately thick substrate (h > W-S in Fig. 2) and Fouad-Hanna's formula [5] is only approximate. However, if Gupta's and Fouad-Hanna's formulas are used for coplanar lines on arbitrary homogeneous substrates, they can yield valid fitting results.

The cross sectional area of the stripline conductors should also be optimized. Thicker striplines provide good current capacity (low series resistance) in the striplines, but increasing the thickness also increases the capacitance. The finite-thickness stripline is modeled as a capacitor in series with the gap capacitance. As a result, the effective gap size decreases and, conversely, the effective width of the stripline increases. Thus, the characteristic impedance will deviate from the originally designed value of 50Ω when the electrode thickness is considered. In this paper, Fouad-Hanna's expression [5] is modified using Gupta's formula [4] to include the effects mentioned above. The

modified expression for characteristic impedance of a coplanar stripline with finite substrate thickness is given by [5]

$$Z_0 = 120\ \pi K(k_e)/K'(k_e)(\epsilon_{eff}{}^t)^{1/2}, \qquad (3)$$

where Z_o is the characteristic impedance, $\epsilon_{eff}{}^t$ is the effective dielectric constant of coplanar stripline, K(k) is the complete elliptic integral of the first kind, K'(k) = K(k') and $k^2=1-k'^2$. It is possilbe to evaluate Z_0 using the following expressions:

$$\epsilon_{eff}{}^t = \epsilon_{eff} - 1.4(\epsilon_{eff}-1)t/[1.4t + SK'(k)/K(k)] \qquad (4)$$

$$\epsilon_{eff}{}^{-1} = (\epsilon_r-1)K(k')K(k_1)/[2K(k)K(k_1')] \qquad (5)$$

$$\Delta = (1.25t/\pi)[1+\ln(4\pi W/t)] \qquad (6)$$

$$d_e = d - \Delta \quad , \quad W_e = W + \Delta, \qquad (7)$$

$$k = a/b, \quad k_e = a_e/b_e, \quad a= S/2 + W, \quad b_e = d_e/2 + W_e \qquad (8)$$

$$k_1 = \sinh(\pi a_e/2h)/\sinh(\pi b_e/2h), \qquad (9)$$

$$\begin{aligned} K(k)/K'(k) &= \pi/\ln[2(1+k'^{1/2})/(1-k'^{1/2})] \quad 0\le k\le 0.7 \\ K(k)/K'(k) &= \pi/\ln[2(1+k^{1/2})/(1-k'^{1/2})] \quad 0.7\le k\le 1.0 \end{aligned} \qquad (10)$$

where S is the gap size, W is the width of the stripline, h is the thickness of the substrate, and t is the thickness of the stripline. We found the width W of the stripline on GaAs corresponding to a 50 Ω characteristic impedance to be 28.6 μm for a 3 μm gap width S.

The thickness of the stripline is closely related to the loss of the device. There are two types of losses in the stripline, conduction loss and dielectric loss. Dielectric losses are normally very small compared with conductor losses for dielectric substrates such as semi-insulating GaAs which has a high resistivity, and can be neglected. Conductor loss, when the quasi-static approximation is valid, can be calculated by considering incremental inductance for evaluating ohmic losses. In general, a thicker stripline provides lower conductor losses [7].

EXPERIMENTAL RESULTS

Our initial design uses 3 μm gaps and 28 μm wide striplines to form a 5 cm long, 50 Ω transmission line, as illustrated in Fig. 2. The electrode mask was produced using our in-house laser scanning system. The striplines are about 0.9 μm thick and consist of 0.6 μm of gold on a Ni-Au/Ge base

which is annealed to form ohmic contact with the substrate. Light modulated at microwave frequencies is coupled into the stripline gap to produce electron-hole pairs. The resulting photoconductive current flow produces a microwave signal on the transmission line.

The device is mounted on an aluminum plate which is especially designed for the test. The bottom side of the plate is removed to prevent the electric field from reflecting back at the surface of the aluminum plate. A 50 Ω copper coaxial cable with a subminiature SMA connector (OSSM connector), which is specified to have flat frequency response to 35 GHz, is chosen to make it possible to reach both electrode pads. The conductors and grounds of the copper cables are connected to both electrode pads with silver epoxy.

Phase matching of the optical and microwave signals is accomplished with an optical delay line arrangement, as in Fig. 3. An Ortel SL 1010 laser diode is modulated by a microwave signal, and light from the laser is divided into four optical beams using a nonpolarizing beam splitters and mirrors. The microwave phase delay of each beam path is expressed as

$$\phi = 2\pi f_m nl/c \tag{11}$$

where n is the refractive index of the medium, l is the length of the beam path, f_m is the microwave frequency, and c is the velocity of light in free space. For phase matching of the optical and microwave signals, the phase difference between any two beam paths should be equal to zero, which means the optical time delay in air must be same as the microwave time delay in the coplanar stripline. The condition for phase matching can be expressed as

$$n_1 \delta l_i = n_2 \delta d_i, \tag{12}$$

where n_1 is the optical refractive index in air (1.00), n_2 is the effective microwave refractive index of the GaAs substrate (2.7), and δl_i and δd_i are, respectively, the path length differences between adjacent optical "spots" in air and in the coplanar stripline. In the experiment, δl_i = 21.6 mm and δd_i = 8 mm.

The Ortel SL 1010 laser diode (I_{th} = 6.6mA), which emits at a wavelength of 0.837 μm, is driven by a dc current of 11 mA. The laser output power is directly modulated by the signal from an HP 8340A microwave synthesized sweeper, coupled to the laser through a bias tee. The power level of the input modulation signal is around -14 dBm. A 9V bias is applied to the electrodes of the TW photodetector with a 12 KΩ series current-limiting resistor, also coupled through a bias tee. The light from the laser is collimated and split

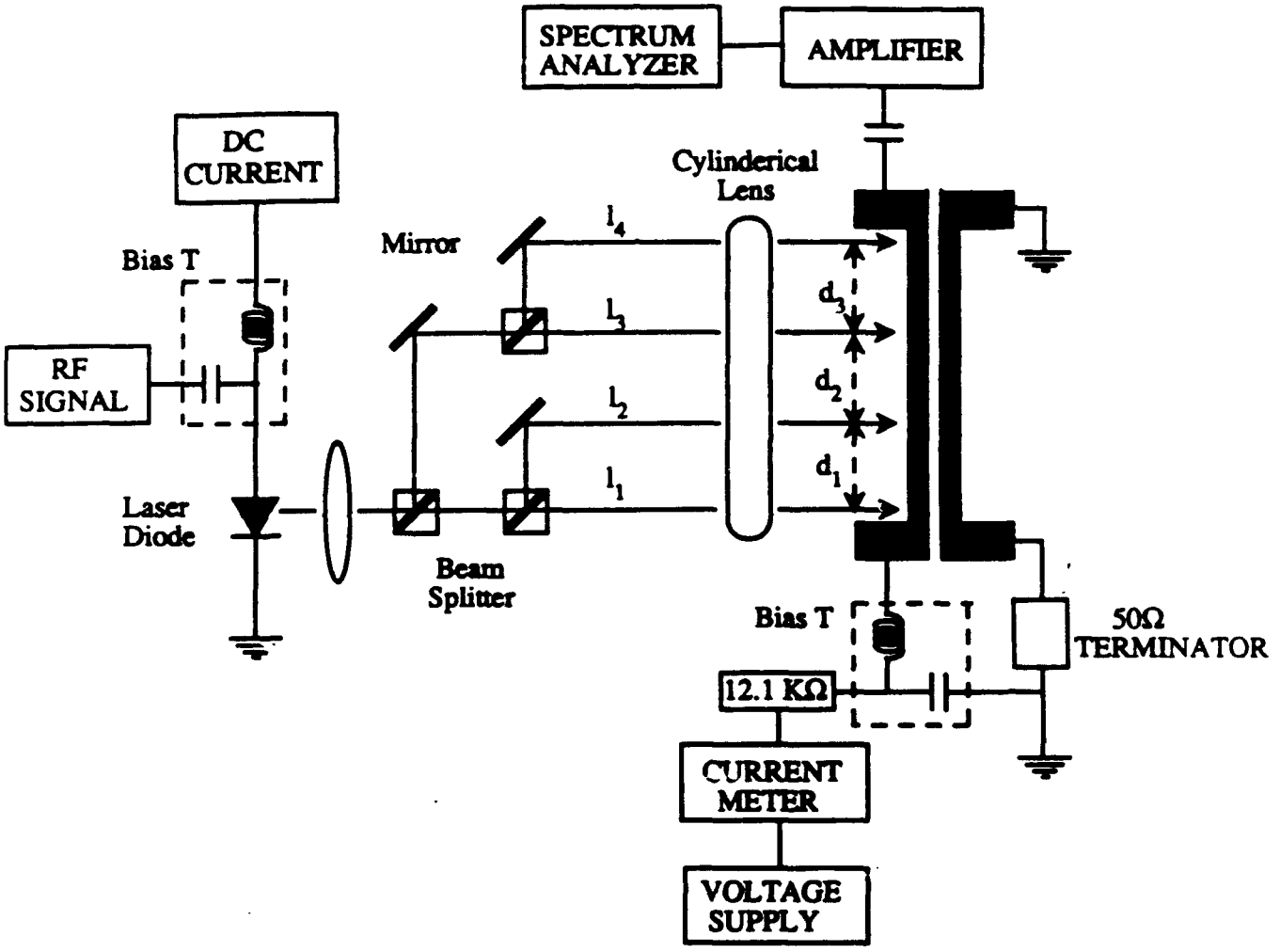

Fig. 3. Experimental arrangement for testing the TW photodetector with four optical inputs.

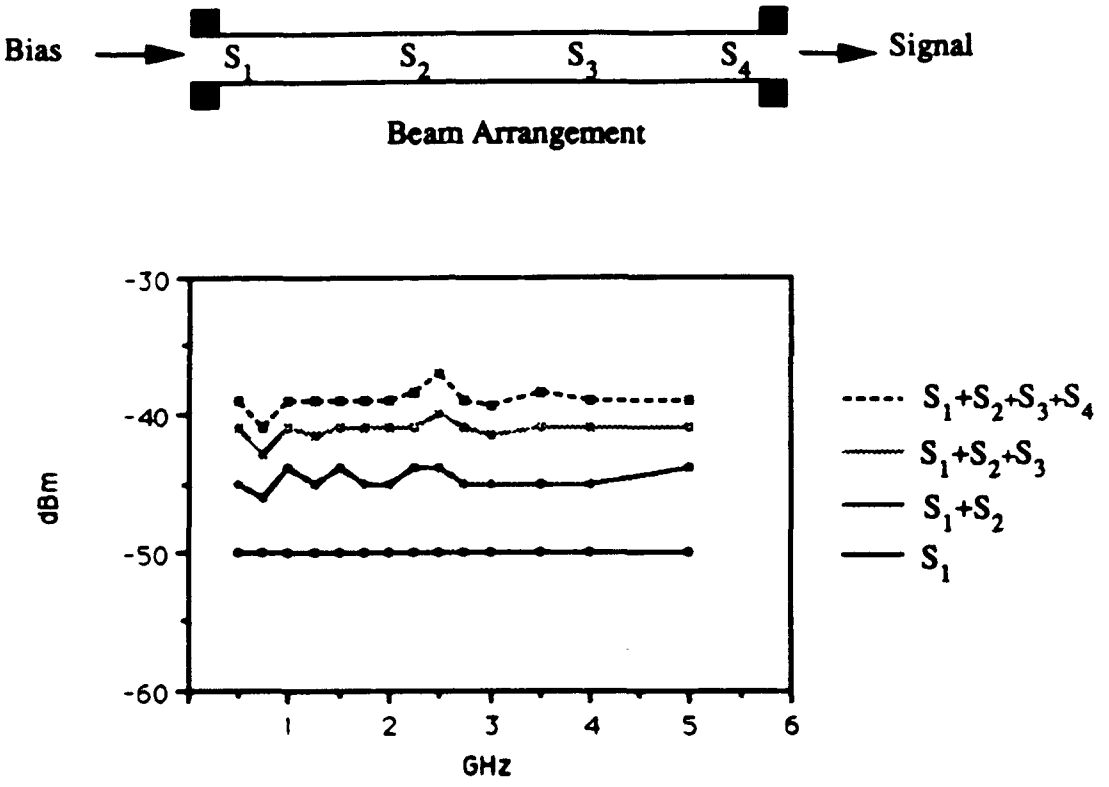

Fig. 4. Response of TW photodetector for the phase-matched case with 1, 2, 3, and 4 optical inputs.

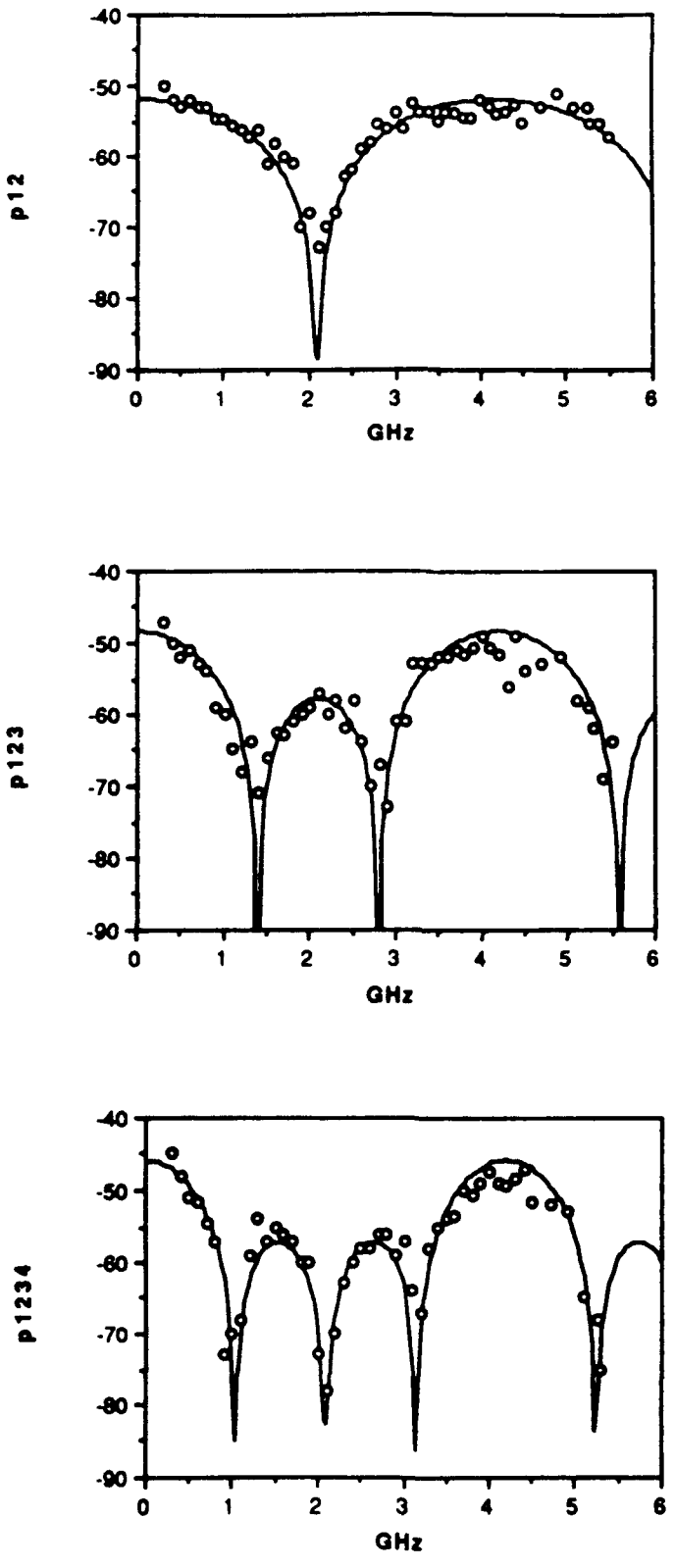

Fig. 5. Response of TW photodetector for the phase-mismatched case with 2, 3, and 4 optical inputs.

into four beams by beam splitters and mirrors. These beams are then focused into the gap region between the stripline conductors using a cylindrical lens as shown in Fig. 3. The microwave signal coming from the bias tee connected to the other electrodes is monitored with an HP 8565A spectrum analyzer as the modulation frequency is varied. For each individual spot the microwave signal level is adjusted to be -50 dBm, over the frequency range from 0.5-5.0 GHz. The spectrum analyzer output is shown in Fig. 4.

Since each beam path is aligned so that the optical signal in air and the microwave signal in the coplanar stripline are in-phase, the output power of the signal becomes independent of the operation frequency and increases as the number of the optical signal inputs is increased. The total output for ideal beam combining can be expressed in dBm as

$$dBm_{N\ inputs} = dBm_{single\ input} + 20\ \log_{10} N, \qquad (13)$$

where N is the number of the optical inputs. As can be seen in Fig. 3, the output power increases by an average of 5.3 dB for N = 2, 8.6 dB for N = 3, and 10.8 dB for N = 4. These are only slightly less than the ideal theoretical values of 6.0 dB for N = 2, 9.5 dB for N = 3, and 12.0 dB for N = 4. It is evident from Fig. 4 that the power output of the combined beams is almost frequency independent, indicating that excellent phase matching of the optical inputs with the microwave signal has been obtained.

To observe the interference effect due to multiple optical input signals when the optical and microwave signals are not phase matched, the same measurement set-up has been used except that the connections for the bias tee and the HP 8565A spectrum analyzer have been reversed. Now, the microwave signal output propagates in the opposite direction from the traveling wave optical excitation. According to equation (11), two adjacent optical inputs have a relative phase delay $\delta\phi$ given by

$$\delta\phi = 2\pi f_m(n_1\delta l_i + n_2\delta d_i)/c, \qquad (14)$$

with c the free-space velocity of light. For the case of N inputs, the response can be written as

$$dBm_N = dBm_1 + 20\ \log_{10}\ [(\sin^2 N\delta\phi/2)/(\sin^2\delta\phi/2)]. \qquad (15)$$

Response peaks occur for $\delta\phi = 2M\pi$, with M an integer. In terms of the microwave frequency at which this occurs, we find that

$$f_m = cM/(n_1\delta l_i + n_2\delta d_i) \qquad (16)$$

The results for two, three, and four optical inputs are plotted in Figs. 5 (a), (b), and (c), respectively. The

theoretical plots of the microwave output for the three cases indicated are also plotted in Fig. 5. For these plots, values for the parameters in eqs. (14) and (15) are $n_1 = 1.0$, $\delta l_i = 4.8$ cm, $n_2 = 2.7$, $\delta d_i = 0.8$cm. We find from eq. (16) that the fundamental frequency (maximum microwave output) occurs for $f_m = 4.3$ GHz.

Another photodetector structure under investigation makes use of an optical waveguide formed a seiconductor substrate, as in Fig. 6. When modulated light from this laser is coupled into the waveguide, electron-hole pairs are created in this layer as the light propagates down the waveguide. This provides a traveling wave excitation of the transmission line at the modulation frequency. Experimental investigations have been carried out in waveguides formed in GaAlAs epitaxial layers on a semiinsulating GaAs substrate, as in Fig. 7. The epitaxial layers were grown for us by Dr. Y. C. Kao of Texas Instruments. A rib waveguide 6 μm wide were formed in the layered sample by reactive ion etching. A coplanar stripline formed on the surface of the sample makes ohmic contact with the top epitaxial layer (GaAs, 0.2 μm thick). Strong optical waveguiding and a photoconductive effect has been observed, as indicated by the response data of Fig. 8 for bias voltages of 0.25, 0.5, and 1.0 V. This data was obtained by endfire coupling of the light from a Ti:sapphire laser into the waveguide. The peak photocurrent is observed at wavelengths greater than 0.86 μm, as indicated by the spectral response curve of Fig. 8. The photoresponse is weak at the 0.83 μm wavelength of our Ortel laser diode, so that no data on the high-speed response chatracteristics were otained for this device.

CONCLUSIONS AND RECOMMENDATIONS

A traveling wave (TW) photodetector with a coplanar stripline structure was designed. The optimum stripline gap width for a focussed Gaussian beam input was determined to be 3 μm. A stripline width of 28 μm was calculated to give a characteristic impedance of 50 Ω as needed to interface the TW photodetector with other microwave circuit elements.

Devices of this type were fabricated in semiinsulating GaAs, using lift-off photolithographic techniques for pattern definition. Ohmic Au/Ge/Ni contacts were formed by a thermal annealing process.

Testing was accomplished using an optical delay line arangement to achieve either matching or mismatching of the microwave phases of the optical inputs and microwave output signal.

For the phase matched case, the observed average microwave output power over the frequency range 0.5 - 5 GHz was 10.8

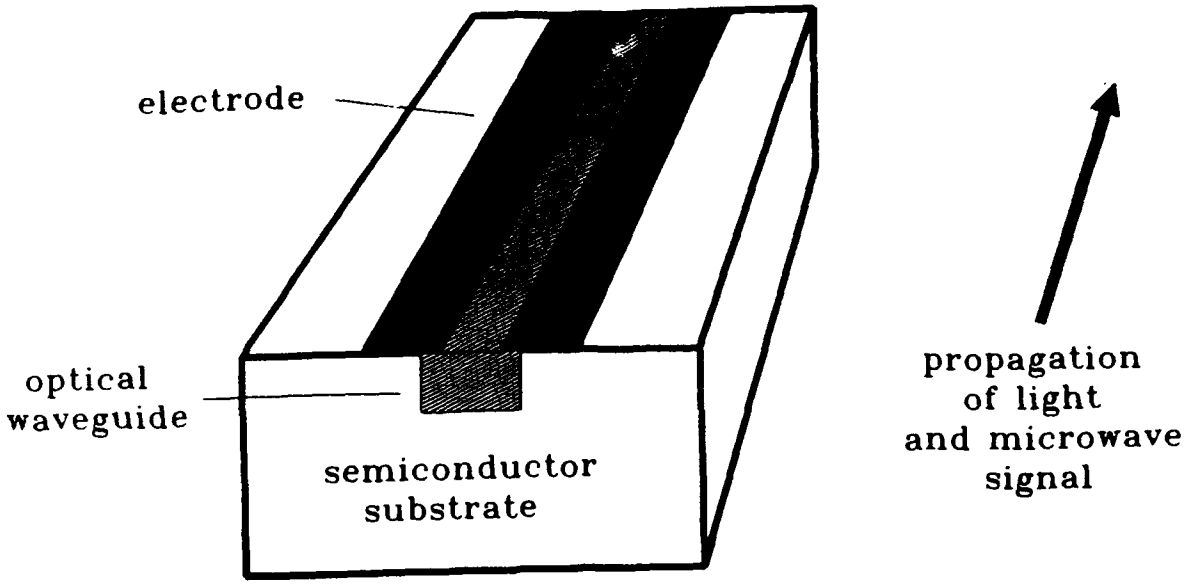

Fig. 6. Optical waveguide configuration for TW photodetector.

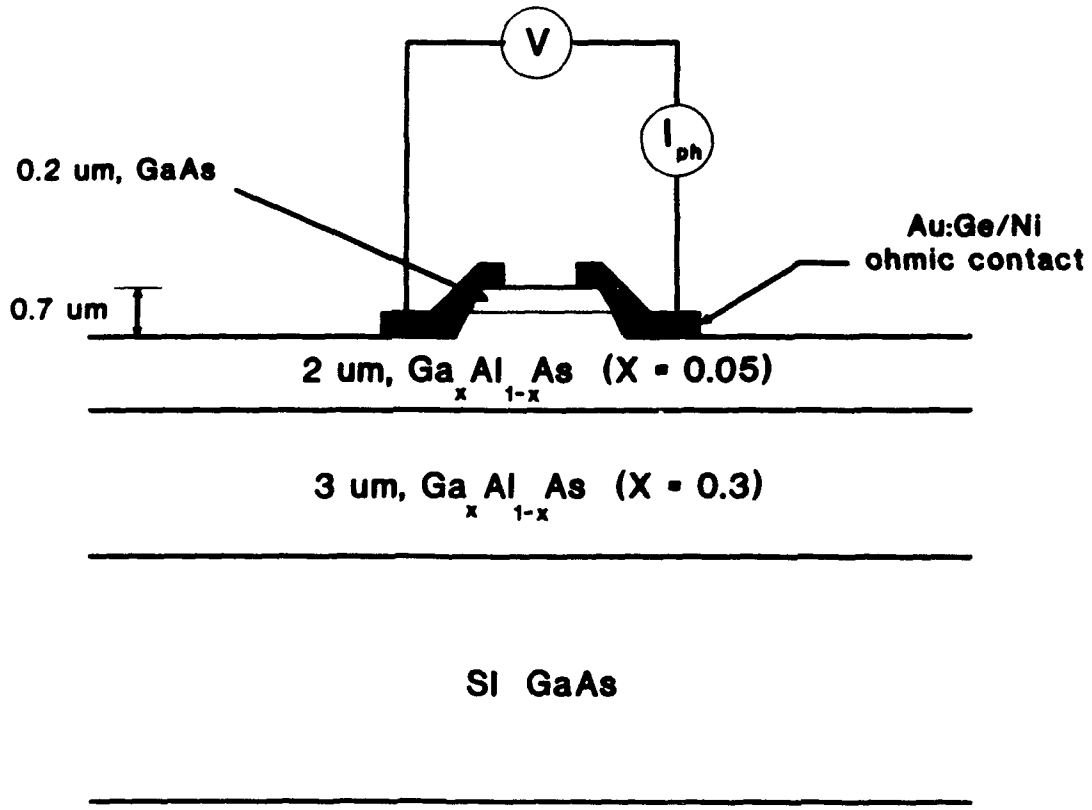

Fig. 7. Cross-section of optical waveguide in AlGaAs.

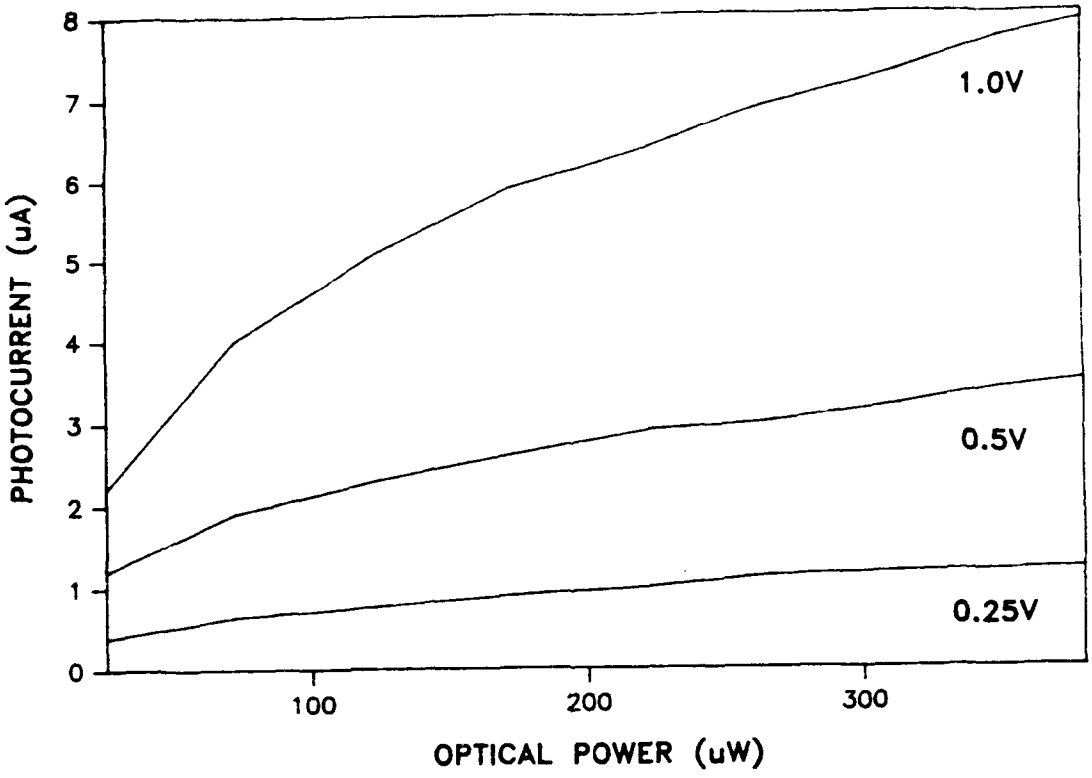

Fig. 8. Dependence of photocurrent on optical power at a wavelength of 0.9 μm.

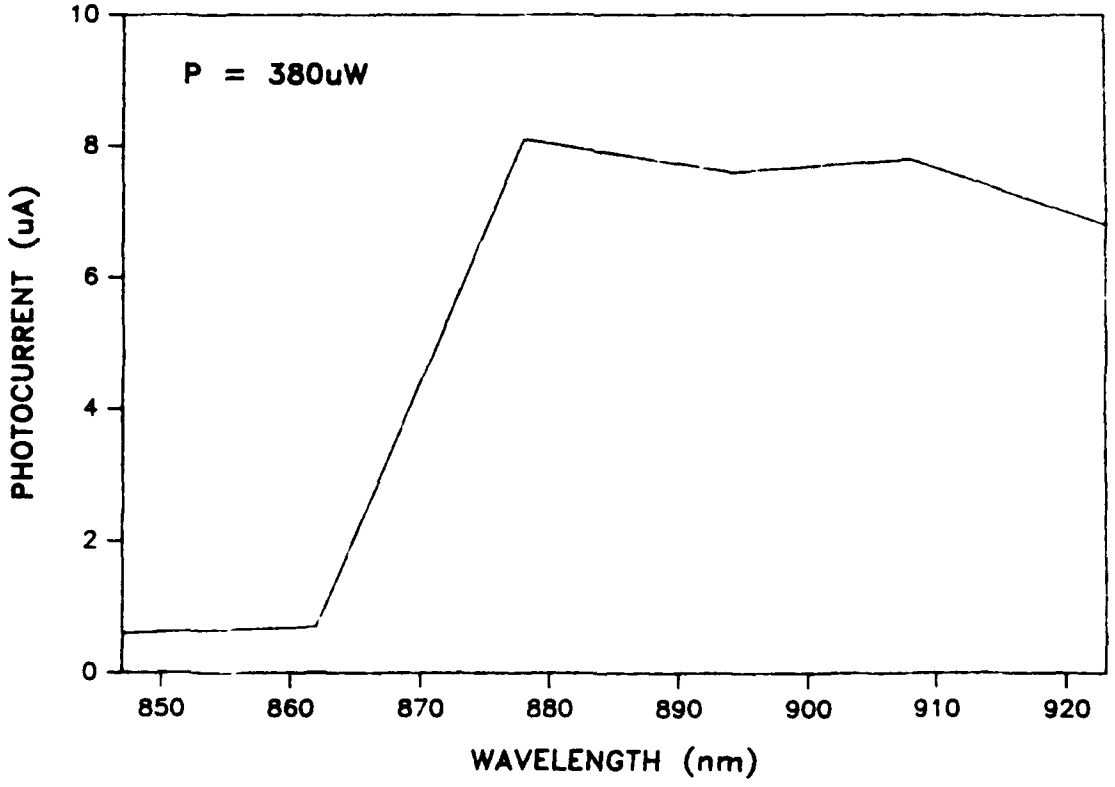

Fig. 9. Spectral response of TW photodetector at 1.0 V bias.

dB for four identical inputs, vs. an ideal value of 12 dB. In this case, optical excitation occurs in distributed fashion along the length of a transmission line structure so that the active area can be much larger than that of lumped-element design, without limitation on the response speed due to the RC time constant.

For the unmatched case, a fundamental frequency of 4.3 GHz was observed for two, three, or four inputs. The expected sidelobe pattern was seen in each case. Here, the TW photodetector performs the function of a transversal filter, which can perform matched filtering and correlation functions with GHz-bandwidth signals. Such performance is possible because the optical input signals are electrically isolated from one another. This would not be possible in an all-electrical analog of this device.

The TW detectors studied to date under this program have used photoconductivity as the optical-to-microwave transduction mechanism. However, carrier lifetime limits the speed of photoconductive devices with near-unity quantum efficiency to less than 10 GHz. For performance in the millimeter-wave regime (30 - 300 GHz), a depleted structure (pn junction or Schottky diode) is needed. Design considerations are considerably different than for photoconductive TW detectors. For example, in the junction devices the junction capacitance per unit length is the critical factor in determining transmission line impedance.

It is recommended that a traveling wave photodetector structures be integrated with a FET amplifier to provide enhanced optical-to-microwave conversion efficiency. One of the TW electrodes can form the gate and the other the drain of the FET. The source and drain of the FET can provide a coplanar line for transmitting the amplified microwave output.

It is also recommended that TW photodetectors based upon pn junction or Schottky diode structures be fabricated in suitable epitaxial material on semiinsulating GaAs substrates. Such structures offer the best prospect for millimeter-wave response in OEIC devices.

Finally, it is recommended that a setup for generating a beat frequency from two high-power laser diodes be assembled and used in future evaluation of the TW photodetectors. With such an arrangement, it should be possible to obtain effective modulated optical power levels of several mW and to demonstrate greatly improved optical-to-microwave conversion efficiencies and dynamic range.

REFERENCES

1. H. F. Taylor, O. Eknoyan, C. S. Park, K. N. Choi, and K. Chang, "Traveling Wave Photodetectors," Proc. SPIE, vol. 1217, pp. 59-63, 1990.

2. D.H. Auston, "Impluse Response of Photoconductors in Transmission Lines", IEEE J. Quantum Electron., vol. QE-19, pp. 639-648, 1983.

3. C.P. Wen, "Coplanar Waveguide: A Surface Strip Transmission Line Suitable for Nonreciprocal Gyromagnetic Device Applications", IEEE Trans. Microwave Theory Tech., Vol. MTT-17, pp. 1087-1090, 1969.

4. K.C. Gupta, R. Garg, and I.J. Bahl, Microstrip Lines and Slotlines, (Artech House, Dedham, MA, 1979) Chapt. 7.

5. V.F. Hanna, "Finite Boundary Corrections to Coplanar Stripline Analysis", Electron. Lett., vol. 16, pp. 604-606, 1980.

6. P.A.J. Dupuis and C.K. Campbell, "Characteristic Impedance of Surface-strip Coplanar Waveguide", Electron. Lett., vol. 9, pp. 354-356, 1973.

7. N. Uchida, "Design and comparison of single-mode planar and ridge type electro-optic waveguide modulators", Optical and Quantum Electron., vol. 9, pp. 1-13, 1977.

MISSION

OF

ROME LABORATORY

Rome Laboratory plans and executes an interdisciplinary program in research, development, test, and technology transition in support of Air Force Command, Control, Communications and Intelligence (C^3I) activities for all Air Force platforms. It also executes selected acquisition programs in several areas of expertise. Technical and engineering support within areas of competence is provided to ESD Program Offices (POs) and other ESD elements to perform effective acquisition of C^3I systems. In addition, Rome Laboratory's technology supports other AFSC Product Divisions, the Air Force user community, and other DOD and non-DOD agencies. Rome Laboratory maintains technical competence and research programs in areas including, but not limited to, communications, command and control, battle management, intelligence information processing, computational sciences and software producibility, wide area surveillance/sensors, signal processing, solid state sciences, photonics, electromagnetic technology, superconductivity, and electronic reliability/maintainability and testability.